

Hydrochemical zoning: natural and anthropogenic origins of the major elements in the surface water of Taizi River Basin, Northeast China

Yingjie Cao¹ · Changyuan Tang^{1,2} · Gaoming Cao³ · Xingze Wang⁴

Received: 11 May 2015 / Accepted: 17 February 2016 / Published online: 28 April 2016
© Springer-Verlag Berlin Heidelberg 2016

Abstract Discriminating the hydrochemical origins in the polluted rivers is a challenge work due to multiple sources contributing to the river's chemical composition. The Taizi River, as an important tributary of the Liao River, in Northeast China, is flowing through an urban-, industry-, and agriculture-intensive area, and its hydrochemistry has been disturbed by human activities especially in the lower basin. In this study, an extensive analysis has been conducted to evaluate the natural and anthropogenic origins of the hydrochemistry in the Taizi River Basin. Three hydrochemical zones are determined based on hydrological connectivity, land use types and lithology, and the hydrochemistry pattern has changed from Ca-HCO₃ type to Ca-HCO₃-SO₄ type from the upper basin to the lower basin due to increasing areas of agriculture and residence land. Six end members including the rain inputs, sewage discharge, mine drainage, carbonate, silicate and evaporate weathering are discriminated in the

study area by applying a two stage stoichiometric method. The first stage is used to separate the anthropogenic inputs (sewage discharge and mine drainage) by an inversion technique, and the second stage is evaluating the rock weathering contributions from carbonates, silicates and evaporates by a forward method. Chemical budget calculation shows that carbonate weathering and anthropogenic inputs are two important factors controlling the hydrochemistry with contributions of about 52 and 27 % of the TDS, respectively. In addition, the contribution of anthropogenic inputs increases from 20 % in the upper basin to 30 % in the lower basin.

Keywords Hydrochemistry · Natural origins · Anthropogenic inputs · The Taizi River

Electronic supplementary material The online version of this article (doi:10.1007/s12665-016-5469-9) contains supplementary material, which is available to authorized users.

✉ Changyuan Tang
tangchangyuan@gmail.com

- ¹ School of Environmental Science and Engineering, Sun Yat-Sen University, No. 135, Xingang Xi Road, Guangzhou 510275, People's Republic of China
- ² Graduate School of Horticulture, Chiba University, Matsudo 271-8510, Japan
- ³ College of Resource Environment and Tourism, Capital Normal University, Beijing 100037, People's Republic of China
- ⁴ Hydrological office of Liaoyang City, Liaoyang 111000, People's Republic of China

Introduction

Numerous studies of major elements and dissolved loads of larger rivers in China have been carried out to study hydrochemical characteristics, estimate chemical erosion and evaluate long term climatic evolution of the earth (Cao et al. 2015; Chen et al. 2002; Ran et al. 2010; Wu et al. 2008; Xu and Liu 2010; Zhang et al. 1995, 2007, 2011). Natural origins such as rain inputs and rock weathering have been widely discussed and recognized as the most important process controlling the river and groundwater hydrochemistry, while with the development of agriculture and industry, the influence of anthropogenic inputs introduced by human activities have become more and more significant to the river flowing through the urban-, industry-, and agriculture-intensive areas. The research on discriminating both natural and anthropogenic origins of the major elements is

an urgent task in river and groundwater hydrochemistry study (Alexakis 2011; Gamvroula et al. 2011).

Two kinds of end-member mixing model, the forward model (Galy and France-Lanord 1999; Krishnaswami et al. 1999; Mortatti and Probst 2003) and the inverse model (Gaillardet et al. 1999; Ollivier et al. 2010) are widely applied to evaluate the contributions of different reservoirs (end-members) to major ion-chemistry of rivers. For these models, the anthropogenic inputs are usually assumed to be negligible, and Gaillardet et al. (1999) also pointed out that for highly polluted rivers draining densely populated, industrialized and cultivated areas, it is not possible to strictly apply these models (both inverse model and forward model) to discriminate the rock weathering contribution (natural origins) because human activities can dominate the major element chemistry of such rivers. In this study, a two stage method is put forward to evaluate the contributions of different end-members. First, the inverse model is used to discriminate anthropogenic inputs, and then the forward model is used to determine the contributions of rock weathering.

The Taizi River with a drainage area of 13,883 km² is one of the main tributaries of the Liao River in the Northeast China. The land use type shows a large difference between upper basin and lower basin in the study area. In the upper basin, forest takes up most of the area, while the lower basin is an urban-, industry-, and agriculture-intensive area. This spatial pattern of land use types results in significant hydrochemistry changes when the river flows from upstream to downstream. How to discriminate different sources of river hydrochemistry in this polluted-river is a challenge in river hydrochemistry studies. A positive attempt has been made by Roy et al. (1999) in the Seine River, France to unravel the contributions of rock weathering, agriculture and communal effluents to river hydrochemistry using an inverse method, and the method is also adopted here to study the natural and anthropogenic origins of the river hydrochemistry in the Taizi River Basin.

In this study, an extensive analysis has been conducted on the major element chemistry to evaluate the natural and anthropogenic origins of the hydrochemistry in the Taizi River. First, three hydrochemical zones are determined based on the hydrological connectivity, land use types and lithology. Then the spatial distribution characteristics of hydrochemistry and the mechanisms controlling the major element chemistry are discussed. The contributions of different end-members (rain inputs, carbonate, silicate and evaporate rock weathering and anthropogenic inputs including mining drainage and domestic sewage) to the river's hydrochemical composition are determined based on a two stage stoichiometric method. Finally, the hydrochemistry evolution along the main channel is discussed.

Study area

The Taizi River, one of the main tributaries of the Liao River, is located in the Liaoning Province in northeast China (Fig. 1). The river originates in the Changbai Mountains and travels from northeast to southwest. Main channel of the Taizi River with a length of 413 km is connected by a large number of tributaries. Digital elevation model (DEM) data shows that the Taizi River Basin is a high mountain area in the east, low plain in the west, and low highland between the mountain area and the plain.

The Taizi River is located in temperate continental monsoon climate zone with hot rainy summer, sunny cold winter and short spring and autumn. Mean annual air temperature, with a range of 2.27–9.99 °C, decreases gradually from downstream to upstream. The temperature is about 22–24 °C in July, and the temperature in January varies between –9 and –17 °C. The annual precipitation ranges from 655 to 954 mm. The annual potential evapotranspiration ranging from 734 to 1018 mm has inverse spatial characteristic compared with the precipitation, as high in the west and low in the east. The average annual runoff of the Taizi River is about 2.69×10^{10} m³.

Main rock types in the Taizi River Basin are composed of gneiss, granite, limestone and sandstone (Fig. 1). In the upper basin, Achaean (a geologic eon between Hadean and Proterozoic) metamorphic rocks outcrop in the north, and are composed of gneiss and schist. Cambro-ordovician carbonates outcrops in the center along the upstream, including calcite and dolomite; on the other hand, Cretaceous volcanic rocks are found in the south of the upper basin, mainly granite. Carboniferous and Jurassic volcanic rocks scatter between the Cambro-ordovician carbonates and Cretaceous volcanic rocks, while within the lower basin, Quaternary sediments cover most of the area in the northwest, and Metamorphic rocks of Proterozoic era including marbles, schist and granulite mainly outcrop in the southeast.

The Taizi River Basin is an urban-, industry-, and agriculture-intensive area in the northeast of China. Benxi, Anshan and Liaoyang are big industrial cities with population of 1.56, 3.47 and 1.82 million in 2005, respectively. Mining activity is also abundant, and 95 % of the total iron mines in the Liaoning Province are distributed in the study area. Another important mineral resource is magnesite which has been considered to have influence on the local hydrochemistry.

Materials and methods

Fifteen (15) surface water samples from the main channel (labeled by “M”) and twenty (20) samples from the major tributaries (labeled by “T”) were taken by field surveys

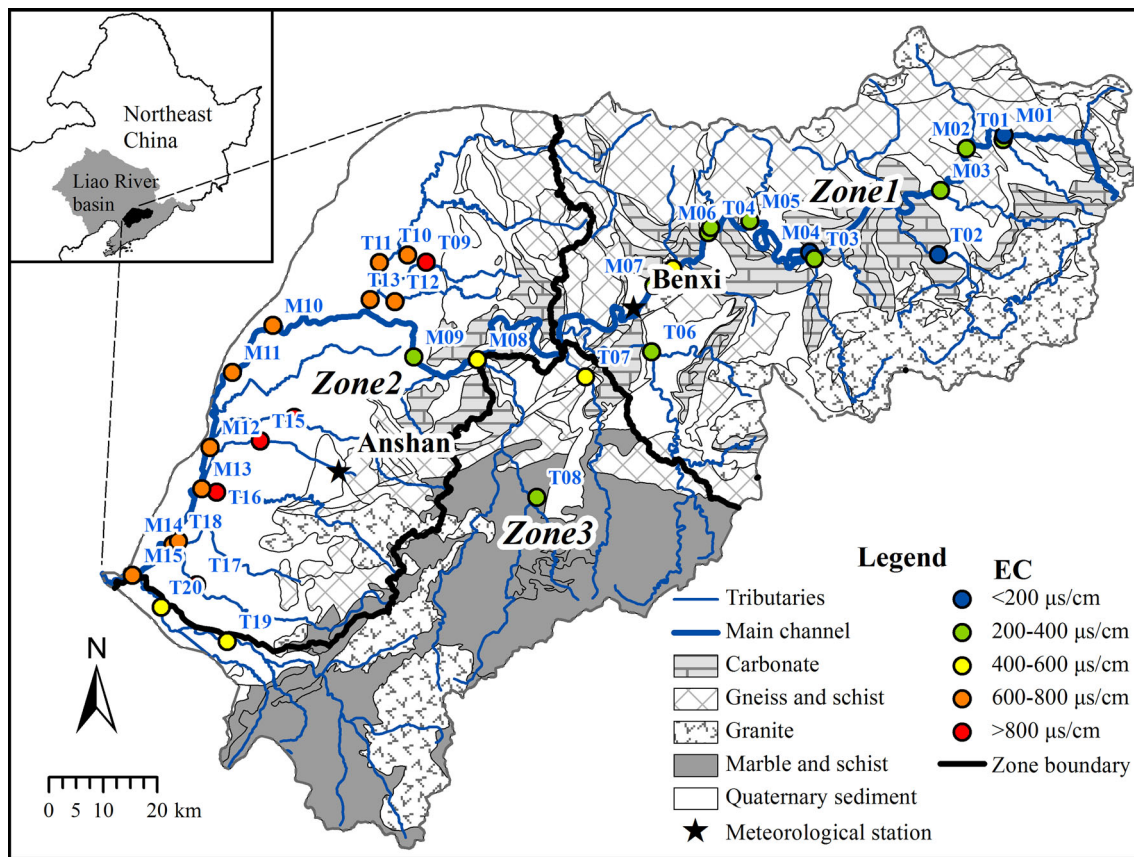


Fig. 1 Sampling points, lithology, spatial distribution of EC and hydrochemical zoning in the Taizi River Basin

from 21 Aug, 2012 to 3 Sep, 2012 (Fig. 1). The river water was sampled by a portable organic class water sampler along the middle thread of channel. Electric conductivity (EC), pH, temperature (T) and dissolved oxygen (DO) were measured by a Horiba U-50 Multiparameter Water Quality Meter, and alkalinity (HCO_3^-) was measured in unfiltered water samples by titration in site. The EC, pH and ORP probes of water quality meter were calibrated by a sodium chloride standard solution ($1990 \pm 10 \mu\text{s/cm}$), pH buffer solution (pH 4.0, 7.0 and 10.0) and ORP standard solution (Zobell's solution), respectively. Samples for major elements and isotopes analysis were filtered through $0.45 \mu\text{m}$ glass fiber filter and stored in 50 ml tubes below 4°C . The cations (Na^+ , K^+ , Ca^{2+} , Mg^{2+}) and anions (Cl^- , SO_4^{2-} , NO_3^-) were analyzed by ion chromatography (LC-10AD, Shimazu) with limit of detection (L.O.D) of 0.01 mg/L. The standard solutions used for ion chromatography analysis are provided by Wako Pure Chemical Industries, Ltd. Ion balance (IB) for samples ranged from -2.20% to $+3.06\%$ with an average of $+0.54\%$ except for M14 (IB = $+5.22\%$) and T18 (IB = $+6.23\%$).

Stable isotopes for water ($\delta^{18}\text{O}$ and δD) were determined by laser spectroscopy (DLT-100; Los Gatos

Research Inc.) at the laboratory of Institute of Geographic Sciences and Natural Resources Research, Chinese Academy of Science. The $\delta^{18}\text{O}$ and δD are reported relative to the VSMOW standard.

Meteorological data from two of the meteorological stations named Benxi in the upper basin and Anshan in the lower basin (Fig. 1) were used to describe the hydrological characteristics during the sampling period. The time series of rainfall data used in this study is 57 years (1956–2012) for Benxi station and 61 years (1951–2012) for Anshan station. The rainfall of 2012 observed in Benxi and Anshan station was 1026 and 997 mm, respectively, which were higher than the average annual values (797 mm in Benxi and 723 mm in Anshan). The monthly rainfall of 2012 in both Benxi and Anshan stations (Fig. 2) showed that the highest rainfall occurred in August. So in this study, the sampling period (21 Aug–3 Sep) could be recognized as within high flow season in high flow year.

The map of sampling sites was drawn by the ArcMap 10.2. Other figures including the ternary diagram were drawn by Origin 8.5. The descriptive analysis, *t* test for two independent samples and analysis of variances (ANOVA) were accomplished by SPSS 19.0.

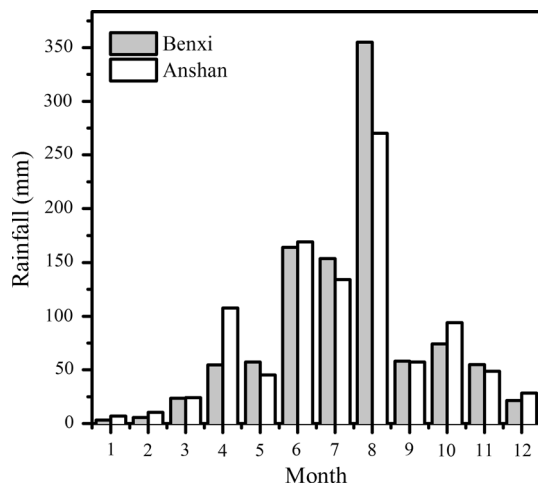


Fig. 2 Month rainfall data of the year of 2012 at two weather stations named Benxi and Anshan

Results and discussion

Overall hydrochemistry characteristics and hydrochemical zoning

Overall hydrochemistry characteristics

Physical parameters and chemical compositions of water samples in the main channel and tributaries of the Taizi River are showed in Table 1. River water in the main channel was slightly alkaline, with pH ranging from 7.6 to 8.0. Electrical conductivity (EC) varied from 195 to 715 $\mu\text{S}/\text{cm}$ (average 421 $\mu\text{S}/\text{cm}$ and median 384 $\mu\text{S}/\text{cm}$). The total dissolved solids (TDS) concentration ranged from 162 to 495 mg/L, and the median was 303 mg/L which was higher than the world median of 65 mg/L (Meybeck and Helmer 1989) and other Chinese rivers such as the Changjiang River (206 mg/L) (Chen et al. 2002), the Pearl River (192 mg/L) (Zhang et al. 2007) and the Huai River (214 mg/L) (Zhang et al. 2011), but lower than the Yellow River (486 mg/L) (Zhang et al. 1995). The tributary water was also slightly alkaline, with pH ranging from 7.6 to 7.9. Electrical conductivity (EC) varied from 140 $\mu\text{S}/\text{cm}$ to over 1000 $\mu\text{S}/\text{cm}$ (average 587 $\mu\text{S}/\text{cm}$ and median 384 $\mu\text{S}/\text{cm}$). The TDS ranged from 105 to 811 mg/L, and the median was 413 mg/L. The highest TDS was observed in two tributaries, the Gexi River (T09, 811 mg/L) and the Yunliang River (T15, 738 mg/L).

Average concentrations of cations (in mg/L) showed that prevalent cations were $\text{Ca}^{2+} > \text{Na}^+ > \text{Mg}^{2+} > \text{K}^+$ for both main channel and tributaries in the Taizi River Basin. In average, calcium was the dominant cation which ranged from 19.2 to 126.9 mg/L with an average of 56.1 mg/L, and accounted for 44–74 % of the cation TDS. The second

abundant cation was Na^+ ranging from 3.81 to 78.2 mg/L with an average of 23.1 mg/L, and it contributed to 7–37 % of the cation TDS. Magnesium varied from 2.4 to 33.4 mg/L with an average of 14.3 mg/L. Potassium was the least cation ranging from 1.0 to 1.8 mg/L with an average of 1.6 mg/L. The average concentrations of major anions (in mg/L) showed that bicarbonate was the dominant anion and was followed by SO_4^{2-} in both the main channel and tributaries. Bicarbonate concentration ranged from 45.8 to 217.2 mg/L with an average of 140.5 mg/L accounting for 30–79 % of the total anions. Sulfate ion ranged from 13.0 to 340.0 mg/L with an average of 86.7 mg/L in the Taizi River, which accounted for 14–58 % of the total anions. Chloride concentration ranged from 2.1 to 99.4 mg/L with an average of 23.4 mg/L. Nitrate concentration ranged from “not detected” to 41.2 mg/L with an average of 18.0 mg/L.

The values of $\delta^{18}\text{O}$ for the samples ranged from -10.5 to -7.1 ‰. The range of δD was from -58.4 to 73.1 ‰.

The *t* test for two independent samples was used here to examine the hydrochemical difference between the main channel and tributaries. Given the significant level $\alpha = 0.05$, it is found that except for SiO_2 , all the hydrochemical parameters have no significant differences implying the tight relationships between the tributaries and main channel. The result of *t* test is attached in supplementary Appendix A.

Hydrochemical zoning

The Taizi River is divided into three zones (Fig. 1) according to the characteristics of hydrological connectivity, land use and lithology. There geographic information system (GIS) layers including sub basin generated by DEM, land use and lithology (geology) layers were used to classifying the watershed by layer overlay function of GIS. First, the watershed was divided into sub basins according to the DEM by Hydrology ArcToolbox in Arcmap 10.2. Then the geology and land use map were applied to merge the adjacent sub basins to make sure each zone has relative uniform lithology and land use types. The characteristics of lithology, land use and average concentrations of major elements for three hydrochemical zones have been showed in Table 1. It is found that the three zones have distinct land use and geology characteristics. Zone 1 which is located on the upper basin is dominated by silicate rocks with an area ratio of 64 %, and its major land use type is forest with an area ratio of 77 %. Zone 2 is located in the west of the lower basin and covered by large area of quaternary sediment (area ratio: 72 %), and its dominant land use type is agriculture with an area ratio of 75 %. Zone 3 is located in the east of the lower basin. Carbonate is the dominant lithology type (area ratio: 61 %) in this

Table 1 Physical parameters, chemical compositions, ion balance and environment isotope ($\delta^{18}\text{O}$ and δD for water) of the Taizi River

ID	T (°C)	EC ($\mu\text{s}/\text{cm}$)	pH	TDS (mg/L)	Na^+ (mg/L)	K^+ (mg/L)	Ca^{2+} (mg/L)	Mg^{2+} (mg/L)	HCO_3^- (mg/L)	Cl^- (mg/L)	SO_4^{2-} (mg/L)	NO_3^- (mg/L)	SiO_2 (mg/L)	Ion balance (%)	$\delta^{18}\text{O}$ (‰)	δD (‰)
M01	22.4	195	7.80	165.73	4.99	1.78	28.56	4.43	90.28	2.75	17.30	11.01	4.63	-0.86	-10.43	-72.93
M02	23.5	207	7.79	169.64	5.21	1.41	29.20	4.80	89.67	2.64	19.36	12.56	4.79	-0.65	-10.31	-71.53
M03	23.2	216	7.81	162.13	5.12	1.92	28.90	4.80	82.35	2.58	19.97	11.78	4.71	2.13	-10.42	-72.86
M04	21.4	200	7.88	164.06	5.10	1.46	29.51	4.54	73.20	3.11	28.54	14.96	3.64	-0.25	-9.06	-66.68
M05	22.7	251	7.83	218.58	6.31	2.01	38.55	5.66	113.46	3.44	31.91	14.00	3.24	-2.20	-9.76	-69.10
M06	21.2	257	7.94	180.60	5.46	1.55	33.49	5.27	81.74	3.15	31.72	14.34	3.88	1.48	-9.97	-68.04
M07	23.1	281	7.97	222.12	7.95	1.99	40.05	6.70	100.04	4.97	41.26	14.84	4.32	1.35	-9.75	-68.71
M08	23.7	427	7.88	338.09	13.30	3.61	57.67	11.49	151.28	12.79	66.62	17.77	3.56	-0.03	-9.34	-67.82
M09	24.0	384	7.93	303.18	16.87	4.26	44.74	13.52	101.26	19.97	85.50	15.81	1.25	-0.62	-7.37	-59.48
M10	26.9	602	7.67	425.90	24.30	5.23	66.97	15.45	157.38	23.7	111.61	17.30	3.96	-0.22	-7.13	-59.32
M11	29.1	604	7.69	436.84	26.14	5.02	68.11	15.29	163.48	24.13	111.55	19.40	3.72	-0.43	-8.85	-64.08
M12	25.0	690	7.66	495.34	36.29	6.28	72.63	18.91	170.80	36.93	127.87	20.24	5.39	0.84	-8.92	-63.61
M13	25.3	654	7.70	454.29	31.56	6.11	68.62	16.61	162.26	31.87	108.93	23.34	4.99	1.12	-9.20	-66.60
M14	25.4	715	7.61	459.68	34.39	10.11	69.01	19.82	170.80	45.49	90.71	12.73	6.62	5.22	-8.51	-67.13
M15	26.5	630	7.83	458.36	29.68	5.89	60.66	22.58	187.88	30.46	91.52	24.02	5.67	0.99	-8.31	-64.74
T01	23.3	280	7.73	240.97	6.70	1.92	42.91	6.42	133.59	2.85	26.83	16.27	3.48	-1.16	-10.49	-73.05
T02	21.6	140	7.93	105.21	3.81	0.96	19.15	2.42	45.75	2.09	13.04	13.99	4.00	1.63	-9.39	-67.20
T03	20.0	207	7.83	175.18	5.67	1.63	31.54	4.80	79.30	3.75	29.17	15.52	3.80	0.04	-9.64	-69.03
T04	25.5	254	7.87	198.65	7.23	2.64	32.96	7.01	90.27	3.53	41.66	8.04	5.31	0.72	-7.57	-63.54
T05	25.1	492	7.66	284.12	5.31	1.32	35.34	5.73	98.00	4.89	32.93	9.83	6.38	-1.56	-9.77	-69.45
T06	21.0	389	7.90	305.59	9.52	3.50	56.18	10.75	115.90	7.81	72.16	25.38	4.39	2.13	-9.04	-66.28
T07	22.0	409	7.89	309.65	8.49	3.18	51.80	11.85	148.84	5.05	58.76	15.93	5.75	-0.43	-10.09	-69.95
T08	23.0	336	7.90	295.00	4.81	2.04	50.44	12.32	156.16	4.99	45.15	14.89	4.20	-0.93	-9.88	-68.22
T09	25.3	1116	7.55	811.37	52.55	7.81	126.9	33.38	178.12	47.26	339.98	20.10	5.27	-0.20	-8.48	-62.58
T10	26.4	655	7.66	447.00	27.39	2.85	73.96	18.4	180.56	38.08	101.44	-	4.32	2.76	-7.60	-58.39
T11	28.1	603	7.69	410.95	28.83	6.48	62.26	15.4	128.10	29.14	111.20	22.48	7.06	1.89	-9.18	-65.04
T12	25.6	771	7.79	577.72	58.70	5.76	72.28	20.17	217.16	28.84	156.43	14.58	3.80	0.81	-7.85	-60.73
T13	27.0	630	7.67	431.99	30.59	6.07	64.76	16.42	161.04	28.35	118.77	-	5.99	1.49	-9.64	-69.97
T14	23.5	829	7.64	616.28	58.32	8.06	80.44	25.01	162.26	58.94	180.88	33.24	9.13	1.28	-8.01	-62.32
T15	26.8	1114	7.56	738.32	78.21	20.38	100.87	21.91	178.12	99.38	211.09	17.76	10.60	1.83	-8.80	-66.47
T16	24.5	802	7.65	568.09	46.88	10.12	76.32	22.69	156.16	51.12	156.21	41.77	6.82	0.48	-9.08	-66.05
T17	26.4	850	7.64	573.77	55.82	9.60	70.13	23.49	196.42	72.96	113.43	24.62	7.30	0.63	-9.00	-65.33
T18	25.2	764	7.56	458.85	33.79	10.33	69.92	21.42	154.94	49.48	95.97	16.06	6.94	6.23	-8.07	-62.62
T19	25.7	534	7.82	405.68	15.26	3.59	53.49	24.57	180.56	14.91	67.96	38.64	6.70	0.54	-9.30	-67.28
T20	27.9	565	7.79	415.69	17.05	4.28	54.58	27.71	176.90	16.89	75.59	36.54	6.15	3.06	-9.39	-66.79

The samples from main channel are labeled by "M" and the samples from tributaries are labeled by "T". The label "-" means that the ion is not detected in water samples

Table 2 Characteristics of geology, land use and average concentrations of major element for three hydrochemical zones

Item	Zone 1	Zone 2	Zone 3
Area ratio of lithology (%)			
Carbonate	20.34	8.02	61.32
Silicate	63.79	19.72	27.31
Quaternary sediment	15.87	72.26	11.37
Area ratio of land use (%)			
Agriculture	16.59	75.22	3.07
Forest	77.27	22.7	94.74
Grass	1.54	0.06	0
Water	1.88	1.56	2.15
Residence	2.73	0.46	0.04
Average values of major element (mg/L)			
TDS	199.45	500.33	356.50
Na ⁺	6.03	37.98	11.40
K ⁺	1.85	7.44	3.27
Ca ²⁺	34.33	72.57	52.58
Mg ²⁺	5.64	19.55	19.11
HCO ₃ ⁻	91.81	165.45	165.61
Cl ⁻	3.66	40.49	10.46
SO ₄ ²⁻	31.22	132.21	61.87
NO ₃ ⁻	14.04	18.96	26.50

The carbonate includes carbonate and marble; the silicate includes granite, sandstone, gneiss and schist. The area of each zone was calculated by the area calculation tool in ArcMap 10.2

zone, and its major land use type is forest with an area ratio of 95 %. According to the geology and land use differences, Zone 1 is defined as silicate-dominated zone; Zone 2 is defined as urban-, industry-, and agriculture-intensive zone; Zone 3 is defined as carbonate-dominated zone.

The average concentrations of major elements of three zones are also showed in Table 2. On average, the samples from Zone 1 had low TDS with an average of 199 mg/L. Calcium comprised 69 % of cation TDS (in meq/L) and HCO₃⁻ comprises 61 % of anion TDS (in meq/L). Due to the influence of human activities, the concentrations of major element in Zone 2 increased greatly. Its average TDS was about 503 mg/L, and the hydrochemistry pattern changed into Ca-HCO₃-SO₄, showing that SO₄²⁻ has become the most abundant anion. In Zone 3, the average TDS (377 mg/L) was higher than Zone 1 while lower than Zone 2. Its dominant cation and anion were Ca²⁺ and HCO₃⁻ mainly due to the chemical weathering of carbonate.

Mechanisms controlling the hydrochemistry and chemical budget

Rain inputs, anthropogenic inputs and rock weathering are treated as major mechanisms controlling the

hydrochemistry. For highly polluted rivers draining densely populated, industrialized and cultivated areas, it is difficult to discriminate the rock weathering contribution because human activities (anthropogenic inputs) can dominate the major element chemistry of such rivers (Flintrop et al. 1996; Gaillardet et al. 1999; Yang et al. 1996). In this study, firstly, the contribution of the rain inputs end members to hydrochemistry is evaluated by chemical features of rain. The $\delta^{18}\text{O}$ and δD for water is applied to determine concentration factor due to evaporation. Then, a three end-members mixing model (an inverse model) is applied to calculate the anthropogenic inputs. At last, the chemical compositions of pristine river have been recalculated by eliminating the rain inputs and anthropogenic inputs. A forward model is applied on the recalculated chemical compositions to evaluate the rock weathering contributions. A detailed description of the methodology for end-members contribution and chemical budget calculation is showed in supplementary Appendix C.

Rain inputs

Rainwater has been recognized as an important source of dissolved species in surface water (Appelo and Postma 2005; Gibbs 1970; Negrel et al. 1993; Stallard and Edmond 1981). The contribution of rain inputs to dissolved salt loads in rivers is expected to be estimated by Cl-normalized ratios of rainwater when there are no terrestrial sources of this element (Negrel et al. 1993). However, in the Taizi River Basin, elevated Cl⁻ concentrations with an average of 23.38 mg/L (0.69 mmol/L) show significant terrestrial sources such as evaporate weathering and anthropogenic inputs existed in the Taizi River, so the Cl-normalized ratios of rainwater cannot be used here to give an estimation of the contribution of rain inputs. In this study, $\delta^{18}\text{O}$ and δD were analyzed to determine the evaporation loss of river waters at the sampling time, and the method used followed the work of Gonfiantini (1986). Based on the calculation, at the sampling time, the evaporation loss ranged from about 0.2 to 20.13 % in the study area (Fig. 3). In addition, the evaporation losses in the lower basin were higher than that in the upper basin. This trend is in agreement with the spatial distribution of the potential evaporation in the Taizi River. (Yi et al. 2010) reported the chemical data of rain at the Shangdianzi regional background station which is located near our study area. The chemical data of rain used in this paper is attached in supplementary Appendix D. The contributions of rain inputs to major element for Zone 1–Zone 3 are showed in Table 3. It is found that as a whole the rain inputs contributed about 2.80 % of Na⁺, 24.33 % of K⁺, 5.11 % of Ca²⁺, 4.80 % of Mg²⁺, 13.30 % of Cl⁻,

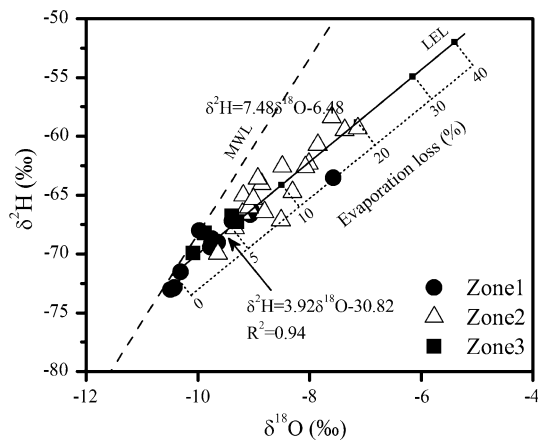


Fig. 3 Relation between $\delta^{18}\text{O}$ and δD of the surface water samples in the Taizi River Basin. *Dash line* shows the local meteoric water line (LMWL) based on the data from Global Networks of International Precipitation Stations (IAEA). *Solid line* gives the linear fit of the evaporation line. The *evaporation line* is determined based on the work of Gonfiantini (1986)

24.84 % of SO_4^{2-} and 25.47 % of NO_3^- at the sampling time. Furthermore, the percentages of rain inputs decreased from Zone 1 in upper basin to Zones 2 and 3 in lower basin due to the combined effects of lithology (rock weathering) and anthropogenic inputs.

Anthropogenic inputs

Two main characteristics of much polluted rivers are that (1) TDS is greater than 500 mg/L and (2) the Cl^-/Na^+ molar ratio is greater than that of sea salts (about 1.16) (Gaillardet et al. 1999). The average TDS in Zone 2 is 500 mg/L, so the samples from Zones 2 are treated as polluted water samples. Some samples from Zones 1 and 3 with high TDS are also treated as polluted water samples. In the study area, domestic sewage and mine drainage have been recognized as two possible anthropogenic inputs to local hydrochemistry due to the urbanization and mine industry development.

The comparison of T08 and T19 in Zone 3 allows us to determine the hydrochemical characteristics of domestic sewage end-member. The draining area of the two tributaries where T08 and T19 were sampled have the same lithology of marble, so that Ca^{2+} and HCO_3^- are the ions showing the least pronounced changes. In fact, similar Ca^{2+} and HCO_3^- concentrations were observed at T08 (Ca^{2+} , 50.44 mg/L; HCO_3^- , 156.16 mg/L) and T19 (Ca^{2+} , 53.49 mg/L; HCO_3^- , 180.56 mg/L) (Table 1). However, land use types for the two sampling points are different. Major land use type of the draining area controlled by T08 is forest and no significant anthropogenic inputs are introduced into this tributary. While for T19, it is located

on the downstream of an intensive residence area and considerable domestic sewage discharge into the river. Therefore the chemical composition of T08 is treated as a representative of natural water end-member which is influenced by rock weathering. The hydrochemical difference between T08 and T19 is used to describe the hydrochemical characteristics of domestic sewage end-members. This method is mainly referring to the work of Roy et al. (1999). In Roy’s work, the hydrochemistry characteristics of anthropogenic end-member was determined by comparing hydrochemistry in two sampling sites with similar lithology but different land use types.

According to the comparison, it is found that increases of 212 % for Na^+ , 222 % for Cl^- , 199 % for NO_3^- and 57 % for SO_4^{2-} were observed at T19 comparing with T08. Increases for Na^+ , Cl^- , NO_3^- and SO_4^{2-} are considered as the inputs from domestic sewage discharge. The Na-normalized molar ratios for K^+ , Ca^{2+} , Mg^{2+} , HCO_3^- , Cl^- , SO_4^{2-} and NO_3^- of the end members of natural water and the domestic sewage are showed in Table 4. It is pointed out that the molar concentrations used in the ratio calculation are corrected by eliminating the rain inputs. From Table 4, it is found that $\text{HCO}_3^-/\text{Na}^+$ and $\text{SO}_4^{2-}/\text{Na}^+$ have the most significant discriminating ability to separate the domestic sewage from the natural water and are selected to depict hydrochemical characteristics of domestic sewage end-member. The hydrochemical characteristics of another end-member, mine drainage, are characterized as extreme low $\text{HCO}_3^-/\text{Na}^+$ (0.01) and extreme high $\text{SO}_4^{2-}/\text{Na}^+$ (300) according to the chemical composition of typical acid mine drainage (AMD) (Oltas et al. 2004).

The hydrochemical compositions of samples used to calculate the $\text{HCO}_3^-/\text{Na}^+$ and $\text{SO}_4^{2-}/\text{Na}^+$ ratios have been eliminated the influence of rain input by deducting the rain origin salts determined in “Rain inputs”. The positions of the end-members and samples are showed in Fig. 4. In the diagram, the mixings of two end-members are represented by the dash lines. All the samples of Zone 2 are located towards the domestic sewage end-member. Some of the samples from Zones 1 and 3 are also located in the area defined by the three end-members, which implies slight deterioration of surface water samples in Zones 1 and 3.

The contributions of domestic sewage (DS) and mine drainage (MD) end-members to Na^+ , Cl^- and SO_4^{2-} of samples are estimated by the mixing equations used by (Ollivier et al. 2010). For example, the mixing equations of Na^+ are listed as bellow:

$$\left(\frac{\text{HCO}_3}{\text{Na}}\right)_{\text{riv}} = \left(\frac{\text{HCO}_3}{\text{Na}}\right)_{\text{DS}} (\alpha_{\text{Na}})_{\text{DS}} + \left(\frac{\text{HCO}_3}{\text{Na}}\right)_{\text{MD}} (\alpha_{\text{Na}})_{\text{MD}} + \left(\frac{\text{HCO}_3}{\text{Na}}\right)_{\text{natural}} (\alpha_{\text{Na}})_{\text{natural}}$$

Table 3 Mean ratios of rain inputs to major ions for 3 hydrochemical zones

Rain inputs (%)	Na ⁺	K ⁺	Ca ²⁺	Mg ²⁺	Cl ⁻	SO ₄ ²⁻	NO ₃ ⁻
Zone 1	5.14	41.40	7.32	8.60	27.94	45.39	31.61
Zone 2	1.01	12.33	3.66	2.54	3.05	11.09	22.55
Zone 3	3.28	22.87	4.48	2.62	11.88	19.89	18.62
Mean	2.80	24.33	5.11	4.80	13.30	24.84	25.47

The ratios is calculated in meq/L

Table 4 Na-normalized molar ratios for K⁺, Mg²⁺, HCO₃⁻, Cl⁻, SO₄²⁻ and NO₃⁻ of the end members of natural water and the domestic sewages

	K ⁺ /Na ⁺	Mg ²⁺ /Na ⁺	HCO ₃ ⁻ /Na ⁺	Cl ⁻ /Na ⁺	SO ₄ ²⁻ /Na ⁺	NO ₃ ⁻ /Na ⁺
Domestic sewages	0.08	1.07	0.55	0.62	0.48	0.84
Natural water	0.18	2.49	13.02	0.59	1.77	0.89

The ratios are calculated by molar concentrations

$$\left(\frac{\text{SO}_4}{\text{Na}}\right)_{\text{riv}} = \left(\frac{\text{SO}_4}{\text{Na}}\right)_{\text{DS}} (\alpha_{\text{Na}})_{\text{DS}} + \left(\frac{\text{SO}_4}{\text{Na}}\right)_{\text{MD}} (\alpha_{\text{Na}})_{\text{MD}} + \left(\frac{\text{SO}_4}{\text{Na}}\right)_{\text{natural}} (\alpha_{\text{Na}})_{\text{natural}} \times (\alpha_{\text{Na}})_{\text{DS}} + (\alpha_{\text{Na}})_{\text{MD}} + (\alpha_{\text{Na}})_{\text{natural}} = 1$$

where, (HCO₃/Na)_i and (SO₄/Na)_i is the molar ratio measured in the river (i = riv), or assumed for each end-member (i = DS, MD and natural). (α_{Na})_i is the mixing proportions of the Na. Similar method was used to estimate the origins of Cl⁻ and SO₄²⁻. For convince, NO₃⁻ is considered to have a sewage origin from both agricultural and domestic sewage discharge.

The proportions of Na⁺, Cl⁻ and SO₄²⁻ originating from the three end-members (domestic sewage, mine drainage and natural water) for the samples are given in Table 5. The domestic sewage contributes about 55 % of Na⁺, 13 % of Cl⁻ and 24 % of SO₄²⁻ for Zone 1, 89 % of Na⁺, 90 % of Cl⁻ and 57 % of SO₄²⁻ for Zone 2 and 47 % of Na⁺, 39 % of Cl⁻ and 23 % of SO₄²⁻ for Zone 3. The anthropogenic inputs have become an important factor controlling the hydrochemical evolution in the lower basin. The mine drainage mainly contributes SO₄²⁻ to the local hydrochemistry with an average of 3 % for Zone 1, 19 % for Zone 2 and 7 % for Zone 3, respectively. In addition, there are little Na⁺ and Cl⁻ derived from the mine drainage with an average percentage lower than 1 %. The natural origin mainly came from rock weathering will be further discussed in following sections in this study.

Rock weathering

Ternary diagram is employed to give an overall understanding on the water–rock reactions which control the major chemical

compositions of river waters (Fig. 5). In Fig. 5, the concentrations of major cations for all the samples have been corrected by eliminating the rain inputs and anthropogenic inputs. It is found that all the samples are located near the carbonate dissolution corner with the ratio of Ca²⁺+Mg²⁺ higher than 80 %. Specifically, samples from Zones 1 and 2 define a narrow range along the line of Na⁺+K⁺ = 0.125, and Ca²⁺+Mg²⁺ take up of about 87 % of the total cations. In addition, Ca²⁺ ratio decreases from 69 % at M01 to 62 % at M09 with Mg²⁺ ratio increasing from 18 % at M01 to 32 % at M09, which reveals that dolomite dissolution enhance along the upper basin. When the river enters into the lower basin (Zone 2), samples mainly locates along the line of Na⁺+K⁺ = 0.06, and the ratio of Ca²⁺+Mg²⁺ increases into 94 %.

Generally, rock weathering contributions to major element composition of rivers can be interpreted in terms of mixing between three main end-members corresponding to the weathering products of carbonates, silicates and evaporates (Gaillardet et al. 1997; Negrel et al. 1993; Ollivier et al. 2010). The contributions from carbonate weathering correspond to the trend towards high-Ca²⁺ end-member close to the top-right corner, and silicate weathering correspond to the trend toward to high-Na⁺ end-member close to the low-left corner in Fig. 6. In Zone 1, the river water has the lowest molar ratios of Ca²⁺/Na⁺ and Mg²⁺/Na⁺, which make the samples locate toward the silicate weathering end-member. When the river enters into Zone 2, both Ca²⁺/Na⁺ and Mg²⁺/Na⁺ molar ratios become higher showing the enhanced influence of carbonate weathering. However, the highest molar ratios of Ca²⁺/Na⁺ and Mg²⁺/Na⁺ in the Taizi River are still lower than the corresponding ratios of the rivers draining karst areas (Han and Liu 2004; Xu and Liu 2010) due to no tributaries flow through purely carbonate-dominated area.

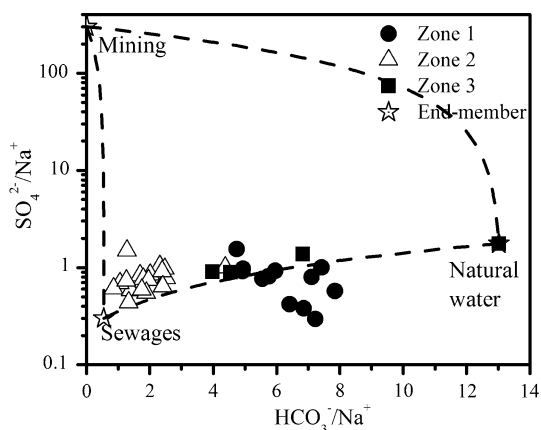


Fig. 4 End-member mixing diagrams using the end-members of sewage discharge, mine draining and natural water expressed by Na-normalized molar ratios. Mixing between two end-members is expressed by the *dash lines*. The mixing lines are round because the log-scales are used for y scale. The molar concentrations used in the ratio calculation are corrected by eliminating the rain inputs

A forward method is applied in this study to determine the contributions of carbonates, silicates and evaporates weathering to the major elements. The molar ratios of Ca^{2+}/Na^+ and Mg^{2+}/Na^+ for silicate weathering are selected as 0.35 and 0.24, respectively (Gaillardet et al. 1999). The concentrations of Ca^{2+} , Mg^{2+} , Na^+ and K^+ are all corrected by eliminating the rain inputs and anthropogenic inputs. The mass balance equations for the calculation are listed as below:

$$\begin{aligned}
 [Ca] &= [Ca_{sil}] + [Ca_{car}] + [Ca_{eva}] \\
 [Mg] &= [Mg_{sil}] + [Mg_{car}] \\
 [Na] &= [Na_{sil}] + [Na_{eva}] \\
 [K] &= [K_{sil}]
 \end{aligned}$$

Table 5 Contributions of anthropogenic inputs (from domestic sewage and mine drainage) and natural origins to Na^+ , Cl^- and SO_4^{2-} in the Taizi River

Zone	Item	Na^+			Cl^-			SO_4^{2-}		
		Sewage (%)	Mining (%)	Natural (%)	Sewage (%)	Mining (%)	Natural (%)	Sewage (%)	Mining (%)	Natural (%)
1	Mean	55.31	0.03	44.67	12.96	0.11	86.93	24.48	3.49	72.03
	Max	66.14	0.25	58.37	56.66	0.59	100.00	33.56	41.39	83.94
	Min	41.63	0.00	33.60	0.00	0.00	42.75	16.06	0.00	38.23
2	Mean	88.81	0.11	11.08	89.84	0.21	9.95	56.68	18.78	24.53
	Max	97.41	0.37	30.76	99.12	0.70	31.09	80.17	62.98	54.22
	Min	69.16	0.01	2.50	68.73	0.03	0.75	30.05	0.00	6.96
3	Mean	47.45	0.06	52.50	38.67	0.17	61.17	22.95	6.59	70.46
	Max	72.43	0.11	100.00	73.80	0.43	95.93	38.25	17.95	99.80
	Min	0.00	0.00	27.50	4.07	0.00	26.06	0.00	0.09	53.62

Because the hydrochemistry data used for anthropogenic inputs calculation has eliminated the influence of rain inputs, the ratios in the table did not include the rain input contributions

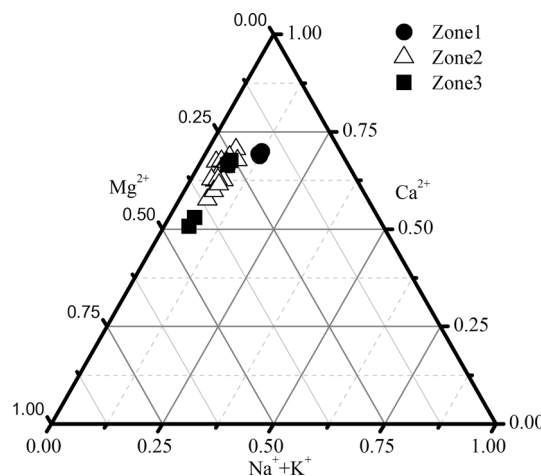


Fig. 5 Ternary diagrams showing the relative abundances (in meq/L) to major cations (Ca^{2+} , Mg^{2+} and $Na^+ + K^+$) in three hydrochemical zones. The major cation concentrations (here in meq/L) used for calculation have been corrected by eliminating the rain and anthropogenic inputs

where, $[Ca]$, $[Mg]$, $[Na]$ and $[K]$ are their concentrations which have been corrected by eliminating the influence of rain and anthropogenic inputs. $[Na_{sil}] = [Na] - [Cl]$, $[Na_{eva}] = [Na] - [Na_{sil}]$, $[Ca_{sil}]/[Na_{sil}] = 0.35$, $[Mg_{sil}]/[Na_{sil}] = 0.24$, $[Ca_{eva}] = [SO_4]$, $[Ca_{car}] = [Ca] - [Ca_{sil}] - [Ca_{eva}]$, $[Mg_{car}] = [Mg] - [Mg_{sil}]$.

The proportions of Ca^{2+} , Mg^{2+} , Na^+ and K^+ originating from different rock weathering reservoirs to the cation TDS originating from rock weathering are illustrated in Fig. 7. Overall, in the Taizi River Basin, 73.84 % of the cations (not including rain inputs and anthropogenic inputs) come from carbonates weathering, and it is the dominating rock weathering factor controlling the local hydrochemistry. Silicate contributes 10.44 % of the cation TDS, and this characteristic

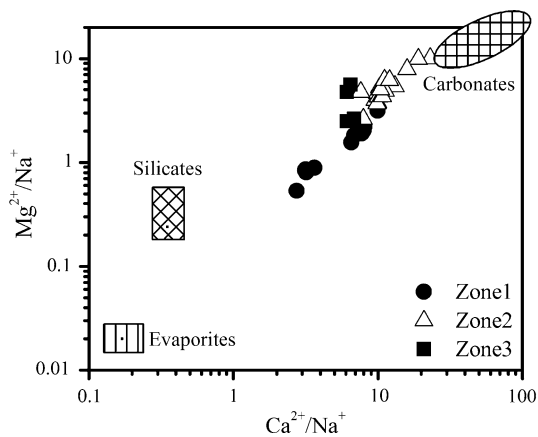


Fig. 6 End-member mixing diagrams using the end-members of carbonates, silicates and evaporates expressed by Na-normalized molar ratios. The cation concentrations (in mmol/L) are all corrected by eliminating rain inputs and anthropogenic inputs

is in agreement with the global silicate weathering proportions (<40.0 %) (Gaillardet et al. 1999). The rock weathering also shows spatial variations, the contribution of carbonate weathering have increased from 67.58 % in upstream to 77.32 % in downstream due to the dissolution of carbonates and disseminated carbonate minerals widely distributed in the Quaternary sediments in the lower basin.

Chemical budget

The chemical budget of rain, anthropogenic and rock weathering inputs to the TDS in the Taizi River are calculated based on the chemical balance method as below, and the result is showed in Fig. 8.

$$\begin{aligned} [Ca] &= [Ca_{rain}] + [Ca_{sil}] + [Ca_{car}] + [Ca_{eva}] \\ [Mg] &= [Mg_{rain}] + [Mg_{sil}] + [Mg_{car}] \\ [Na] &= [Na_{rain}] + [Na_{sil}] + [Na_{eva}] + [Na_{anth}] \\ [K] &= [K_{rain}] + [K_{sil}] \\ [HCO_3] &= [HCO_{3car}] + [HCO_{3sil}] \\ [Cl] &= [Cl_{rain}] + [Cl_{eva}] + [Cl_{anth}] \\ [SO_4] &= [SO_{4rain}] + [SO_{4eva}] + [SO_{4anth}] \\ [NO_3] &= [NO_{3rain}] + [NO_{3anth}] \end{aligned}$$

where $[X_{rain}]$, $[X_{anth}]$, $[X_{car}]$, $[X_{sil}]$ and $[X_{eva}]$ are the contribution of different end-members to element X and have been described in “Mechanisms controlling the hydrochemistry and chemical budget”; $[HCO_{3car}]$ and $[HCO_{3sil}]$ is separated based on the ratio of $([Ca_{car}] + [Mg_{car}])/([Ca_{sil}] + [Mg_{sil}] + [Na_{sil}] + [K_{sil}])$, $[Cl_{eva}] = [Na_{eva}]$.

Based on the calculation, it is found that carbonate weathering is the most important mechanism controlling the local hydrochemistry, and contributes about 51.57 % of

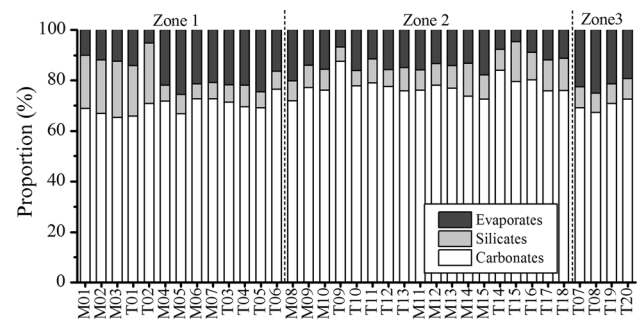


Fig. 7 Calculated contributions (%) of carbonate, silicate and evaporate weathering to the rock weathering cation TDS (without rain and anthropogenic inputs) in the Taizi River Basin. The hydrochemical concentrations used for calculation are expressed in molar concentration (mmol/L)

the TDS in the study area. The second source of TDS is anthropogenic inputs due to sewage discharge and mine draining which contribute about 27.34 % of the TDS. Silicate weathering has the minimum contribution with an average of 4.49 % to the TDS. The contributions of evaporate weathering and rain inputs are considered as 9.66 and 6.93 %, respectively.

On average, the contribution of carbonate weathering shows its maximum value (about 59.80 %) in Zone 3 which has the largest area ratio of carbonate outcrops. The minimum contribution of carbonate is about 47.29 % in Zone 2 where the water hydrochemistry is disturbed significantly by human activities. The contribution of carbonate weathering is decreasing along the main channel from the upstream to the downstream with a rate of +0.33 %/10 km. For the contribution of anthropogenic inputs, it also shows significant spatial variation due to spatial heterogeneity of land use distribution. In Zone 1, anthropogenic inputs take up about 20.20 % of the TDS and show little change along the river. When the river enters into Zone 2, the anthropogenic input rapidly increases into 35.60 %. The ratio is increasing with a rate of +1.40 %/10 km from M08 to the river mouth. The contribution of rain inputs shows a decreasing trend from 10.50 % in the upstream to 4.97 % in the downstream. The contribution of silicate weathering shows a relative small spatial variation with an average of 4.49 % and a SD of 1.22 %. No spatial trend is observed for the contribution of evaporate weathering.

Hydrochemistry evolution

Variations of major elements and saturation index (SI) for gypsum, calcite and dolomite along the main channel and the corresponding tributaries are showed in Fig. 9. It is clear that the concentrations of major elements have a significant increasing trend from upstream to downstream,

and the hydrochemistry along the main channel is controlled by the chemical inputs from the tributaries. This characteristic disagrees with the trends observed in the Changjiang River and the Huai River, where the major elements or TDS concentrations of the main channel showed a general decreasing trend, and the tributaries display the dilution effect to the main channel (Chen et al. 2002; Zhang et al. 2011).

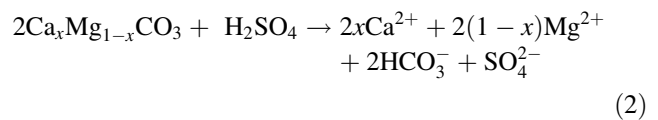
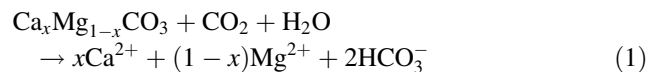
The increasing rates from upstream sampling point M01 to river mouth sampling point M14 for Na⁺, K⁺, Ca²⁺, Mg²⁺, HCO₃⁻, Cl⁻ and SO₄²⁻ are 589, 467, 141, 347, 89, 1554 and 424 %, respectively. An appreciable increase of major element concentrations is observed due to anthropogenic inputs after M07 located near the boundary of Zones 1 and 2 (Fig. 9). The river is unsaturated for calcite and dolomite before M07. After M08, the water becomes oversaturated for calcite and dolomite, and the SI shows slight changes and has an average of 0.31 and 0.40 for calcite and dolomite in the main channel. The water is unsaturated for gypsum along the whole river.

To give a detailed analysis of the hydrochemistry evolution, major ions are divided into two groups based on the hydrochemical origins. One group including Na⁺, Cl⁻ and SO₄²⁻ is significantly influenced by anthropogenic inputs. Based on the chemical budget calculation, in the Taizi River, in molar concentrations, more than 90 % of Na⁺, 55 % of Cl⁻ and 52 % of SO₄²⁻ come from anthropogenic inputs. Only 28 % of Na⁺, 44 % of Cl⁻ and 47 % of SO₄²⁻

have rock weathering origins. The variations of these ions along the main channel show a continuous increase trend due to high solubility.

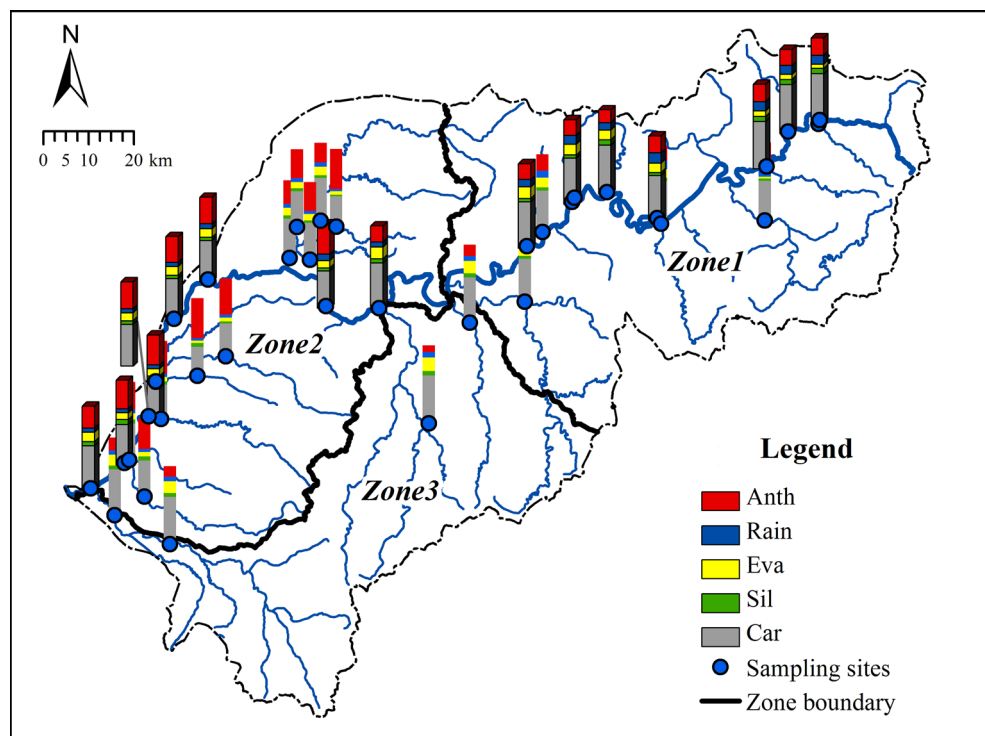
Another group including Ca²⁺, Mg²⁺ and HCO₃⁻ is mainly controlled by carbonate weathering. Two important weathering agents, carbonic acid (CO₂) and sulfuric acid (H₂SO₄) have been recognized as providing protons to the dissolution of rocks (Galy and France-Lanord 1999; Han and Liu 2004; Karim and Veizer 2000; Li et al. 2008; Xu and Liu 2010; Yoshimura et al. 2001). CO₂ is derived directly from the atmosphere and produced by remineralization of organic matter in soil, while H₂SO₄ can be produced through the oxidation of pyrite relating to the mining activity and anthropogenic emissions of SO₂ from coal combustion (Xu and Liu 2010).

When carbonates are weathered by dissolved CO₂ and H₂SO₄, Ca²⁺ and Mg²⁺ can be produced according to the equations (Chetelat et al. 2008; Lerman and Wu 2006) as below:



According to the stoichiometric relations of chemical reactions (1) and (2), for waters that have SO₄²⁻/HCO₃⁻

Fig. 8 Spatial distribution of chemical budget for each sampling point. The hydrochemical concentrations used for chemical budget calculation are expressed in molar concentration (mmol/L)



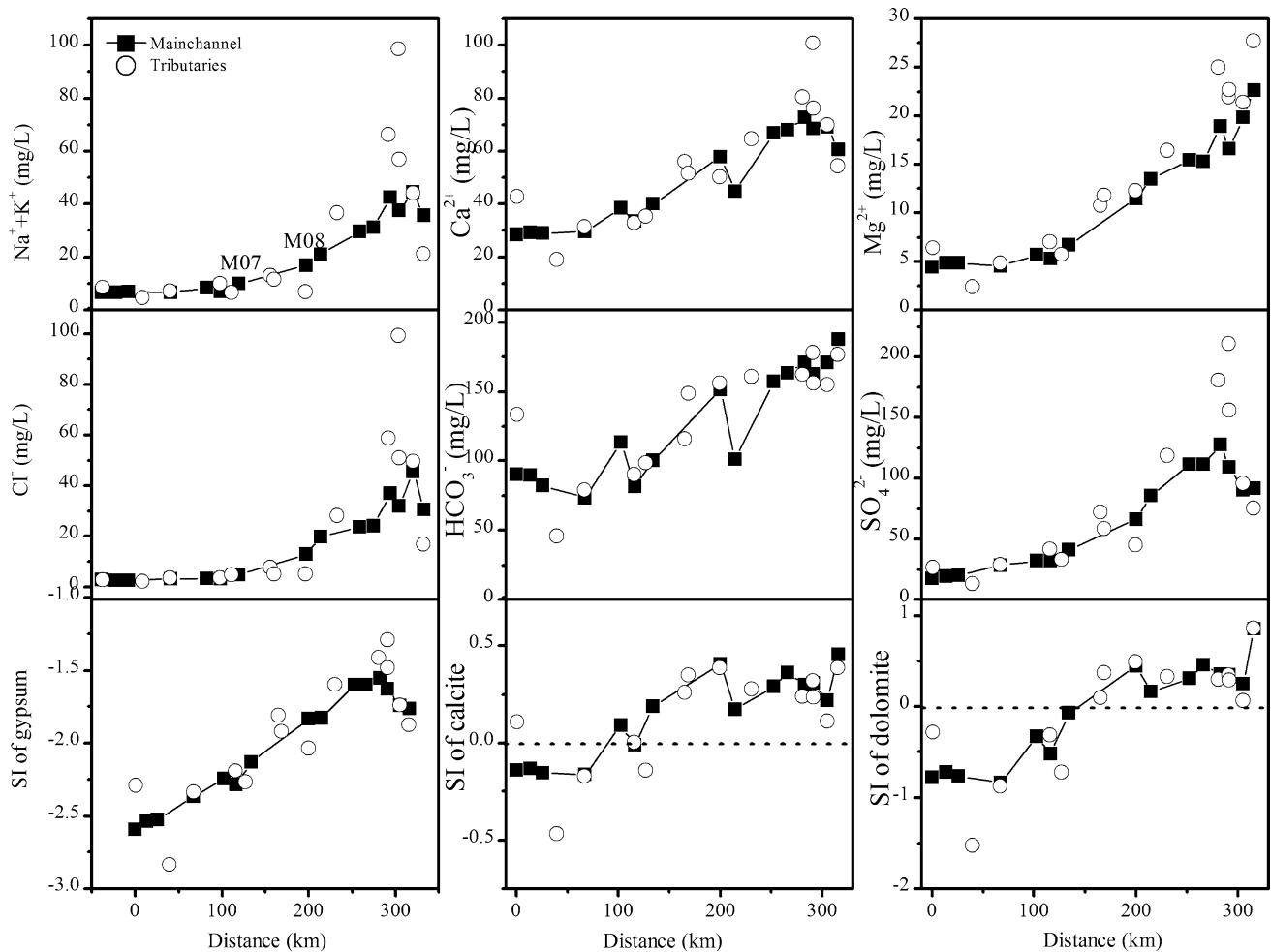


Fig. 9 Variations of major ions and saturation index (SI) for gypsum, calcite and dolomite along the main channel

equivalent ratios around zero, carbonate dissolution by CO_2 dominates the chemical weathering. For water that has $\text{SO}_4^{2-}/\text{HCO}_3^-$ equivalent ratios around 0.5, carbonate dissolution by H_2SO_4 dominates the chemical weathering. When carbonate dissolution by both CO_2 and H_2SO_4 takes place, samples located on the mixing line defined by the two end-members discussed above (Fig. 10). In addition, the locations of the *mixing lines* are influenced by the molar ratio of Ca/Mg in the carbonates, which is represented by $r = x/(1 - x)$. In the study area, the river waters samples locate around the mixing lines (Fig. 10), indicating a mixing between solute from carbonate dissolution by CO_2 and H_2SO_4 . In the upper basin, most of the samples locate on the left side of Fig. 10 with $\text{SO}_4^{2-}/\text{HCO}_3^-$ ratios lower than 0.25, and it is showed that carbonate dissolution by CO_2 dominates in this area. For the lower basin, samples concentrate on the right side with $\text{SO}_4^{2-}/\text{HCO}_3^-$ ratios higher than 0.25 showing that carbonate dissolution by H_2SO_4 become important process controlling the chemical weathering. In addition, Fig. 10 also shows that Ca/Mg

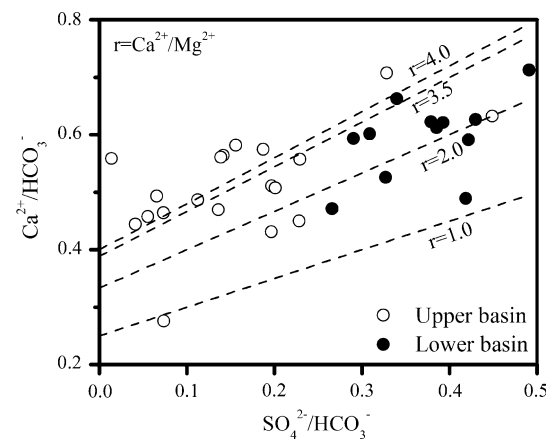


Fig. 10 Relation between molar ratios of $\text{Ca}^{2+}/\text{HCO}_3^-$ and $\text{SO}_4^{2-}/\text{HCO}_3^-$. Molar ratio of $\text{SO}_4^{2-}/\text{HCO}_3^-$ defines the two end members aroused by carbonate weathering by CO_2 and H_2SO_4 . When $\text{SO}_4^{2-}/\text{HCO}_3^- = 0$, carbonate is dissolved by CO_2 according to reaction (1), and when $\text{SO}_4^{2-}/\text{HCO}_3^- = 0.5$, carbonate is dissolved by H_2SO_4 according to reaction (2). The values of r give the Ca/Mg ratio which is calculated by $x/(1 - x)$. Dash lines show mixing lines

ratio of carbonate changes from $r = 3.5$ in the upper basin to $r = 2.0$ in the lower basin due to increasing magnesite in the lower basin.

Conclusions

In this study, the Taizi River Basin has been divided into three hydrochemical zones to analyze the natural and anthropogenic origins of the major elements in the surface water. Among these zones, Zone 2 which is located on the lower basin is considered as human activity disturbing areas comparing with Zones 1 and 2. The hydrochemistry pattern has changed from Ca-HCO₃ type to Ca-HCO₃-SO₄ type from the upper basin to the lower basin due to the increasing areas of agricultural and residence land.

Six end-members (rain inputs, sewage drainage, mine draining, carbonate, silicate and evaporate weathering) are considered to have influences on local hydrochemistry. A two-stage model is put forward to separate the contributions of six end-members. Chemical budget calculation shows that carbonate weathering is the most important factor controlling the local hydrochemistry and contributes about 52 % of the TDS. Anthropogenic inputs contribute about 27 % of the TDS. The sum of the contribution from silicate weathering, evaporate weathering and rain inputs is about 21 %. In addition, the contribution of anthropogenic inputs increases from 20 % in the upper basin to 30 % in the lower basin.

The hydrochemistry evolution in the Taizi River is controlled by carbonate weathering by carbonic acid (CO₂) and sulfuric acid (H₂SO₄) and anthropogenic inputs. In the upper basin, the river is unsaturated for calcite, dolomite and gypsum. When the river enters into the lower basin, it becomes oversaturated for calcite and dolomite, while still unsaturated for gypsum. The river waters samples show a mixing between solute from carbonate dissolution by CO₂ and H₂SO₄. And the increase of magnesite outcrops in the lower basin influence the Ca/Mg ration in the river.

References

- Alexakis D (2011) Diagnosis of stream sediment quality and assessment of toxic element contamination sources in East Attica, Greece. *Environ Earth Sci* 63:1369–1383
- Appelo CAJ, Postma D (2005) *Geochemistry, groundwater and pollution*. CRC Press, Boca Raton
- Cao Y, Tang C, Song X, Liu C (2015) Major ion chemistry, chemical weathering and CO₂ consumption in the Songhua River basin, Northeast China. *Environ Earth Sci* 73:7505–7516
- Chen J, Wang F, Xia X, Zhang L (2002) Major element chemistry of the Changjiang (Yangtze River). *Chem Geol* 187:231–255
- Chetelat B, Liu C, Zhao Z, Wang Q, Li S, Li J, Wang B (2008) Geochemistry of the dissolved load of the Changjiang Basin rivers: anthropogenic impacts and chemical weathering. *Geochim Cosmochim Acta* 72:4254–4277
- Flintrop C, Hohlmann B, Jasper T (1996) Anatomy of pollution: rivers of north Rhine-Westphalia, Germany. *Am J Sci* 296(1):58–98
- Gaillardet J, Dupre B, Allegre CJ, Négrel P (1997) Chemical and physical denudation in the Amazon River Basin. *Chem Geol* 142:141–173
- Gaillardet J, Dupré B, Louvat P, Allegre C (1999) Global silicate weathering and CO₂ consumption rates deduced from the chemistry of large rivers. *Chem Geol* 159:3–30
- Galy A, France-Lanord C (1999) Weathering processes in the Ganges–Brahmaputra basin and the riverine alkalinity budget. *Chem Geol* 159:31–60
- Gamvroula D, Alexakis D, Stamatis G (2011) Assessment of groundwater quality in the Megara basin, Attica, Greece. *Advances in the research of aquatic environment*. Springer, Berlin, pp 393–400
- Gibbs RJ (1970) Mechanisms controlling world water chemistry. *Science* 170:1088–1090
- Gonfiantini R (1986) Environmental isotopes in lake studies. *Handb Environ Isot Geochem* 2:113–168
- Han G, Liu C-Q (2004) Water geochemistry controlled by carbonate dissolution: a study of the river waters draining karst-dominated terrain, Guizhou Province, China. *Chem Geol* 204:1–21
- Karim A, Veizer J (2000) Weathering processes in the Indus River Basin: implications from riverine carbon, sulfur, oxygen, and strontium isotopes. *Chem Geol* 170:153–177
- Krishnaswami S, Singh S, Dalai T (1999) Silicate weathering in the Himalaya: role in contributing to major ions and radiogenic Sr to the Bay of Bengal Ocean Science, trends and future directions, Indian National Science Academy and Akademia International, pp 23–51
- Lerman A, Wu L (2006) CO₂ and sulfuric acid controls of weathering and river water composition. *J Geochem Explor* 88:427–430
- Li S-L, Calmels D, Han G, Gaillardet J, Liu C-Q (2008) Sulfuric acid as an agent of carbonate weathering constrained by $\delta^{13}\text{C}$ DIC: examples from Southwest China. *Earth Planet Sci Lett* 270:189–199
- Meybeck M, Helmer R (1989) The quality of rivers: from pristine stage to global pollution. *Glob Planet Change* 1:283–309
- Mortatti J, Probst J-L (2003) Silicate rock weathering and atmospheric/soil CO₂ uptake in the Amazon basin estimated from river water geochemistry: seasonal and spatial variations. *Chem Geol* 197:177–196
- Négrel P, Allègre CJ, Dupré B, Lewin E (1993) Erosion sources determined by inversion of major and trace element ratios and strontium isotopic ratios in river water: the Congo Basin case. *Earth Planet Sci Lett* 120:59–76
- Olias M, Nieto J, Sarmiento A, Cerón J, Cánovas C (2004) Seasonal water quality variations in a river affected by acid mine drainage: the Odiel River (South West Spain). *Sci Total Environ* 333:267–281
- Ollivier P, Hamelin B, Radakovitch O (2010) Seasonal variations of physical and chemical erosion: a 3-year survey of the Rhone River (France). *Geochim Cosmochim Acta* 74:907–927
- Ran X, Yu Z, Yao Q, Chen H, Mi T (2010) Major ion geochemistry and nutrient behaviour in the mixing zone of the Changjiang (Yangtze) River and its tributaries in the Three Gorges Reservoir. *Hydrol Process* 24:2481–2495
- Roy S, Gaillardet J, Allegre C (1999) Geochemistry of dissolved and suspended loads of the Seine river, France: anthropogenic impact, carbonate and silicate weathering. *Geochim Cosmochim Acta* 63:1277–1292

- Stallard R, Edmond J (1981) Geochemistry of the Amazon: 1. Precipitation chemistry and the marine contribution to the dissolved load at the time of peak discharge. *J Geophys Res Oceans* (1978–2012) 86:9844–9858
- Wu W, Xu S, Yang J, Yin H (2008) Silicate weathering and CO₂ consumption deduced from the seven Chinese rivers originating in the Qinghai–Tibet Plateau. *Chem Geol* 249:307–320
- Xu Z, Liu C-Q (2010) Water geochemistry of the Xijiang basin rivers, South China: chemical weathering and CO₂ consumption. *Appl Geochem* 25:1603–1614
- Yang C, Telmer K, Veizer J (1996) Chemical dynamics of the “St. Lawrence” riverine system: $\delta\text{D H}_2\text{O}$, $\delta^{18}\text{O H}_2\text{O}$, $\delta^{13}\text{C DIC}$, $\delta^{34}\text{S}$ sulfate, and dissolved $^{87}\text{Sr}/^{86}\text{Sr}$. *Geochim Cosmochim Acta* 60:851–866
- Yi L, Xiaolan Y, Hongbing C, Weili L, Jie T, Shufeng W (2010) Chemical characteristics of precipitation at three Chinese regional background stations from 2006 to 2007. *Atmos Res* 96:173–183
- Yoshimura K, Nakao S, Noto M, Inokura Y, Urata K, Chen M, Lin P-W (2001) Geochemical and stable isotope studies on natural water in the Taroko Gorge karst area, Taiwan—chemical weathering of carbonate rocks by deep source CO₂ and sulfuric acid. *Chem Geol* 177:415–430
- Zhang J, Huang W, Letolle R, Jusserand C (1995) Major element chemistry of the Huanghe (Yellow River), China—weathering processes and chemical fluxes. *J Hydrol* 168:173–203
- Zhang S, Lu X, Higgitt D, Chen C, Sun H, Han J (2007) Water chemistry of the Zhujiang (Pearl River): natural processes and anthropogenic influences. *J Geophys Res Earth Surf* 112:137–161
- Zhang L, Song X, Xia J, Yuan R, Zhang Y, Liu X, Han D (2011) Major element chemistry of the Huai River basin, China. *Appl Geochem* 26:293–300